VUV action spectroscopy of protonated Leucine-enkephalin peptide in the 6-14 eV range

M. Lj. Ranković,[1] F. Canon,[2] L. Nahon,[3] A. Giuliani,[3,4] and A. R. Milosavljević[1,5,a)]

[1]*Institute of Physics Belgrade, University of Belgrade, Pregrevica 118, 11080 Belgrade, Serbia*

[2] *INRA, UMR1324 Centre des Sciences du Goût et de l'Alimentation, F-21000 Dijon, France*

[3]*SOLEIL, l'Orme des Merisiers, St Aubin, BP48, 91192 Gif sur Yvette Cedex, France*

[4]*INRA, UAR1008, CEPIA, Rue de la Géraudière, BP 71627, 44316 Nantes, France*

[5]*Radiation Laboratory, University of Notre Dame, Notre Dame, Indiana 46556, USA*

We have studied the VUV photodissociation of gas-phase protonated leucine-enkephalin peptide ion in the 5.7 to 14 eV photon energy range by coupling a linear quadrupole ion trap with a synchrotron radiation source. We report VUV activation tandem mass spectra at 6.7, 8.4 and 12.8 eV photon energies and photodissociation yields for a number of selected fragments. The obtained results provide insights into both near VUV radiation damage and electronic properties of a model peptide. We could distinguish several absorption bands and assign them to particular electronic transitions, according to previous theoretical studies. The photodissociation yields appear to be very different for the various observed fragmentation channels, depending both on the type of fragments and their position along the peptide backbone. The present results are discussed in light of recent gas-phase spectroscopic data on peptides.

I. INTRODUCTION

Investigation of the interaction of Vacuum Ultraviolet (UV) radiation with polymers of amino acids, namely peptides and proteins, is of essential importance. These molecules are ubiquitous in the biosphere and are involved in many important processes in living organisms. Their function and activity are intrinsically connected with their primary structure – the sequence of amino acids [1]. Therefore, any alteration to the primary sequence and degradation of the biopolymer, due to interaction with energetic photons such as UV, Vacuum UV (VUV) or X-rays, may lead to severe consequences and ultimately to cellular death. All these effects are commonly ascribed as radiation damage. In this respect, deep UV and VUV action spectroscopy of biopolymers isolated in the gas phase offers possibilities to investigate photon activation processes of particular mass-to-charge selected systems. Such experiments could help reaching fundamental understanding of the radiation damage at the molecular level.

On the other hand, the availability of third generation synchrotron radiation facilities, providing high-resolution, tunable and high-brightness sources of energetic photons, as well as recent development of state-of-the-art spectroscopic experimental systems, allowed for detailed investigation of electronic and structural properties of biomolecules. However, until recently the VUV spectroscopic and dynamical studies have been limited only to amino acids, since these relatively

small molecules can be evaporated and thus introduced as neutrals into the gas phase (see e.g. [2–4] and references therein), as well as some small peptides [5] and nucleobases [6].

The study of the building blocks of biomolecules is certainly important to understand the physicochemical properties of a biopolymer that they form. However, this bottom-up approach is still insufficient to reach comprehensive knowledge about the complex biological systems such as proteins and DNA. Indeed, the electronic structure and physicochemical properties of biopolymers are built up from the properties of their building units, as well as from the intramolecular interactions closely correlated with their primary, secondary and tertiary structures. For example, in a peptidic chain, amino-acids are connected to each other through peptide bonds, which crucially influence protein's electronic structure. Moreover, biomolecules are not isolated in nature, and solvent can strongly affect their radiation response[7–9]. Therefore, the building blocks approach in the investigations of complex biomolecules may be of limited relevance in some aspects regarding their electronic structure, structural properties, function and radiation damage sensitivity.

The recent development of experimental techniques that couple ion traps with synchrotron radiation sources has opened up possibilities to perform VUV action spectroscopy of protonated or deprotonated large biopolymers isolated in the gas phase [10–13]. The biomolecules are brought into the gas phase by electrospray ionization (ESI) [14], selected and stored in a radio frequency (RF) ion trap. The technique is based on tandem mass spectrometry, where a particular precursor ion is selected, activated by VUV radiation and analyzed using mass spectrometry. A high sensitivity and selectivity of the mass spectrometry, a prolonged interaction time in the trap and a high brightness of third generation SR sources provide respectable signal to noise ratio, overcoming significantly lower target densities in comparison with classic spectroscopy of neutral molecules [12]. The energy tunable SR sources enable recording of tandem mass spectra (MS^2) as a function of the photon energy. Therefore, action spectroscopy of desired target ions is performed by recording photoionization and photofragmentation ion yields.

Leucine-enkephaline (Leu-enk) consists of five amino acids arranged in the following sequence: Tyr-Gly-Gly-Phe-Leu (YGGFL) (see Fig. 1) and has been intensively investigated in recent years to become a standard model in mass spectrometry [15]. Recently, we have also investigated VUV photon interaction with both bare and nanosolvated Leu-enk dimers [16,17]. We have measured the backbone photofragment yields and thus mapped the electronic excitation bands for the Leu-enk dimer molecule that lead to molecular dissociation [17]. More interestingly, we have found a significant stabilization effect of only three water molecules, which has been also confirmed by Density Functional Theory (DFT) calculations [16]. Bari et al. [11] have

reported the pioneering and detailed investigation of the photodissociation of gas-phase protonated Leu-enk trapped cations in the 8 to 40 eV photon energy range. They have discussed in detail photofragmentation patterns both below and above the ionization threshold and presented ion yields for a number of different fragments. However, the latter study [11] was fragmentary regarding the low VUV photon energies below 10 eV, as the authors probed only a few energies in this domain. Therefore, it was not possible to discuss spectroscopic features in the energy range below 10 eV and the corresponding lowest energy electronic transitions of the Leu-enk molecule.

The present study extends previous works on model peptides and Leu-enk [11,16–18] in several directions. It reports novel results of the VUV action spectroscopy of an isolated peptide. This is an extension of our previous work on Substance P peptide (11 residues) [18], investigating the electronic structure of Leu-enk molecule, which is a smaller 5-amino acid peptide with a simpler fragmentation pattern. Therefore, the present work allows for deep insight into general electronic properties of a peptide. On the other hand, we also significantly extend the previous study of VUV-induced energy-dependent fragmentation of Leu-enk molecule [11]. Indeed, this time we dominantly focus on the low-energy VUV domain, where the electronic excitations trigger molecular dissociation.

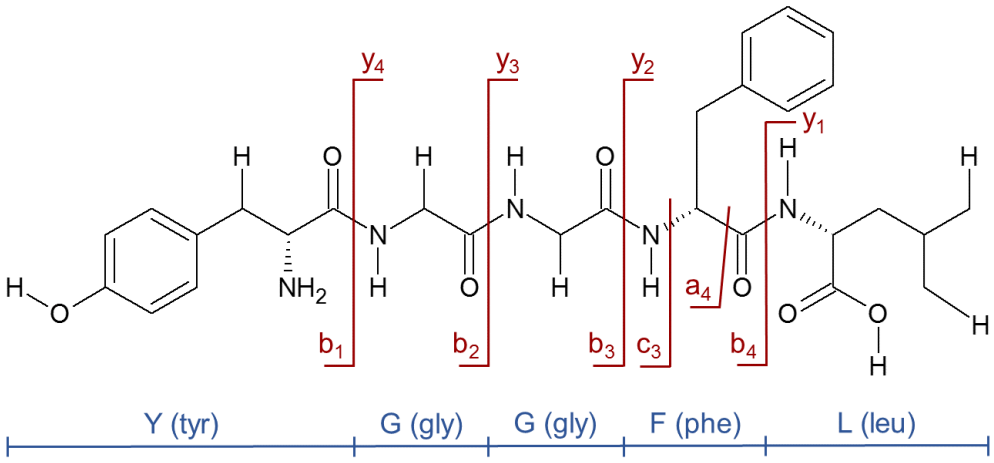

FIG. 1. The structure of Leucine-enkephaline peptide, with its five amino acid constituents and imonium ions with mass-to-charge ratios Y(136), F(120) and L(86).

II. EXPERIMENTAL METHOD

A commercial linear quadrupole ion trap mass spectrometer (Thermo Finnigan LTQ XL) was used both for ion production and selection/isolation. It was previously modified and coupled [10,19] to the VUV beamline DESIRS [20] of the SOLEIL synchrotron radiation facility in France. The front side of LTQ mass spectrometer was equipped with an electrospray ionization (ESI) source. Ions produced by ESI were introduced through the system of ion lenses and stored in the linear ion trap. Singly protonated precursor ions $[\text{Leu-Enk} + \text{H}]^+$ (m/z 556) were selected and stored in the ion trap, where

they were irradiated using monochromatic VUV photon beam for 500 ms. The control of the irradiation time has been achieved, by installing a fast rotating mechanical shutter in the path of the photon beam [21], inside a dedicated vacuum chamber on the back side of LTQ.

The VUV photon beam was produced by an electromagnetic undulator (OPHELIE II) feeding the DESIRS beamline and further monochromatized using a normal incidence monochromator, resulting in a typical bandwidth of 12 meV in the present case [20]. The absolute photon energy uncertainty was a few tens meV, as calibrated against the zero order. A monochromator grating of 200 gr mm^{-1} in combination with 200 μm exit slit was used, allowing for a high photon flux of $10^{12} – 10^{13}$ ph/s. In order to obtain high spectral purity, higher harmonics from the undulator were removed using a Krypton gas filter (cutoff above 14 eV) and MgF_2 window filter (cutoff above 10.6 eV). A pressure difference between the synchrotron beamline (10^{-8} mbar) and the LTQ mass spectrometer (10^{-5} mbar) was accommodated with a custom made differential pumping stage, in assembly with mechanical shutter and a movable photodiode. The later was used to measure the photon flux just before the ion trap. The LTQ mass spectrometer was mounted on a custom-made supporting frame with several degrees of freedom, for rotational and translational position adjustment. A precise alignment of the photon beam with respect to the ion trap axis was essential for achieving high ion activation efficiency and signal to noise ratio.

Leu-enk was provided by Sigma-Aldrich in a powder form and was dissolved in water/acetonitrile (75:25 v/v) mixture at a concentration of 10 μM. After photon activation of the isolated ions, all fragments were ejected from each side of the trap towards detectors, and tandem mass spectrum (MS^2) was recorded for particular photon energy. Each sequence of ion isolation, photon activation and mass spectrum recording was repeated for different photon energies. A home-made PC software was used to control and synchronize the ion isolation, the opening of mechanical shutter, the beamline photon energy adjustment and the mass spectra recording. Automated data acquisition scans lasting up to several hours, resulted in 30-50 mass spectra with 0.2 eV energy step, for a desired precursor.

The photodissociation ion yields were extracted from the recorded mass spectra, by plotting the area under the peak of interest against the photon energy, and normalizing to the photon flux and the total ion current (TIC). The photon flux was measured in a separate energy scans, with a photodiode (AXUV100, International Radiation Detectors) under the same experimental conditions. For the present experiment, two scans of the photon flux were performed, one with Krypton gas filter and one with MgF_2 glass window filter. In order to cover the whole energy range of interest, three separate action scans of $[M+H]^+$ precursor, within partly overlapping energy domains (5.7-8.5) eV, (7.2-10.2) eV and (10-14) eV, were performed.

The first energy range of (5-8) eV was measured with the MgF_2 glass window filter, whereas the other two ranges were measured with the Krypton gas filter. Extraction and normalization of all ion yields has been performed separately for each energy range. The final energy yield for each fragment ion, in the overall range from 5.7 to 14 eV, was obtained by coupling three separately obtained normalized relative ion yields. Additional normalization procedure to couple the lowest energy fragment ion yields (5.7-8.5) eV with the other two was the following. All fragment ion yields in the higher energy ranges (from 7.2-10.2 and 10-14 eV domains), were both multiplied with the independent factor for each fragment ion, to achieve the best overlap with the same fragment ion yield in the lowest energy range. In other words, fragment yields from the two higher ranges were down-scaled to match the yields from the first energy range, each ion fragment having its own scale factor.

III. RESULTS AND DISCUSSION

A. Tandem mass spectrometry

The schematic structure of Leu-enk molecule is presented in Fig. 1. Upon VUV photon absorption, the electronic excitation and the ionization of the precursor, can both induce bond cleavages (photodissociation and dissociative ionization, respectively) leading to different fragment ions. As for peptide backbone cleavage, depending on both which particular bond has been cleaved along the backbone and where the remaining charge stays upon this bond cleavage, there is a standard nomenclature [22,23] of the fragments: a_n, b_n, c_n for N-terminal and x_n, y_n, z_n for C-terminal, where subscripts indicate the number of amino acid residues left in particular fragment. Additionally, the photon absorption can induce detachment of neutral groups (e.g. amino acid residues) and multiple bond cleavages.

Fig. 2 presents the MS^2 obtained at three prominent photon energies: at 6.7 eV (below the ionization threshold), at 8.4 eV (near, just below the threshold) and at 12.8 eV (above the threshold). The ionization energy (IE) of the protonated molecule has been predicted from DFT calculations to be at 8.87 eV [11]. The peak designated at mass-to-charge ratio (m/z) 556 corresponds to the parent cation of protonated Leu-enk $[M+H]^+$. For energies lower than IE (Fig. 2a,b) the fragmentation pattern appears to be very similar to MS^2 recorded in collision-induced dissociation (CID) experiments [15]. At these energies, photo-induced fragmentation mainly proceeds through cleavage of a peptide backbone that yield *a*, *b* and *y* fragments, which are clearly visible in the mass spectrum at 6.7 eV (Fig. 2a). Dominant Leu-enk fragments in the mass spectra recorded at incident photon energies below IE are a_4 (m/z 397), b_3 (m/z 278), y_2 (m/z 279) and b_4 (m/z 425). Fragments assigned to precursor's loss of one water molecule $[M+H]^+$-H_2O (m/z 538) and the tyrosine side chain $[M+H]^+$-107 (m/z 449) are also clearly visible, while precursor's loss of phenylalanine side chain $[M+H]^+$-91 (m/z 465) is of much lower abundance.

Fragments b_3 (m/z 278) and y_2 (m/z 279) could not be separated in the previous VUV photodissociation study [11], but are clearly resolved in the present mass spectra (see the inset in Fig. 2a). Further internal fragmentation of a_4 and b_4 can lead to fragments with ammonia loss a_4-NH_3 (m/z 380), loss of glycine a_4-NH_3-57 (m/z 323), loss of tyrosine side chain b_4-107 (m/z 318), GGF (m/z 262), GF (m/z 205) and loss of carbon monoxide GF-CO (m/z 177).

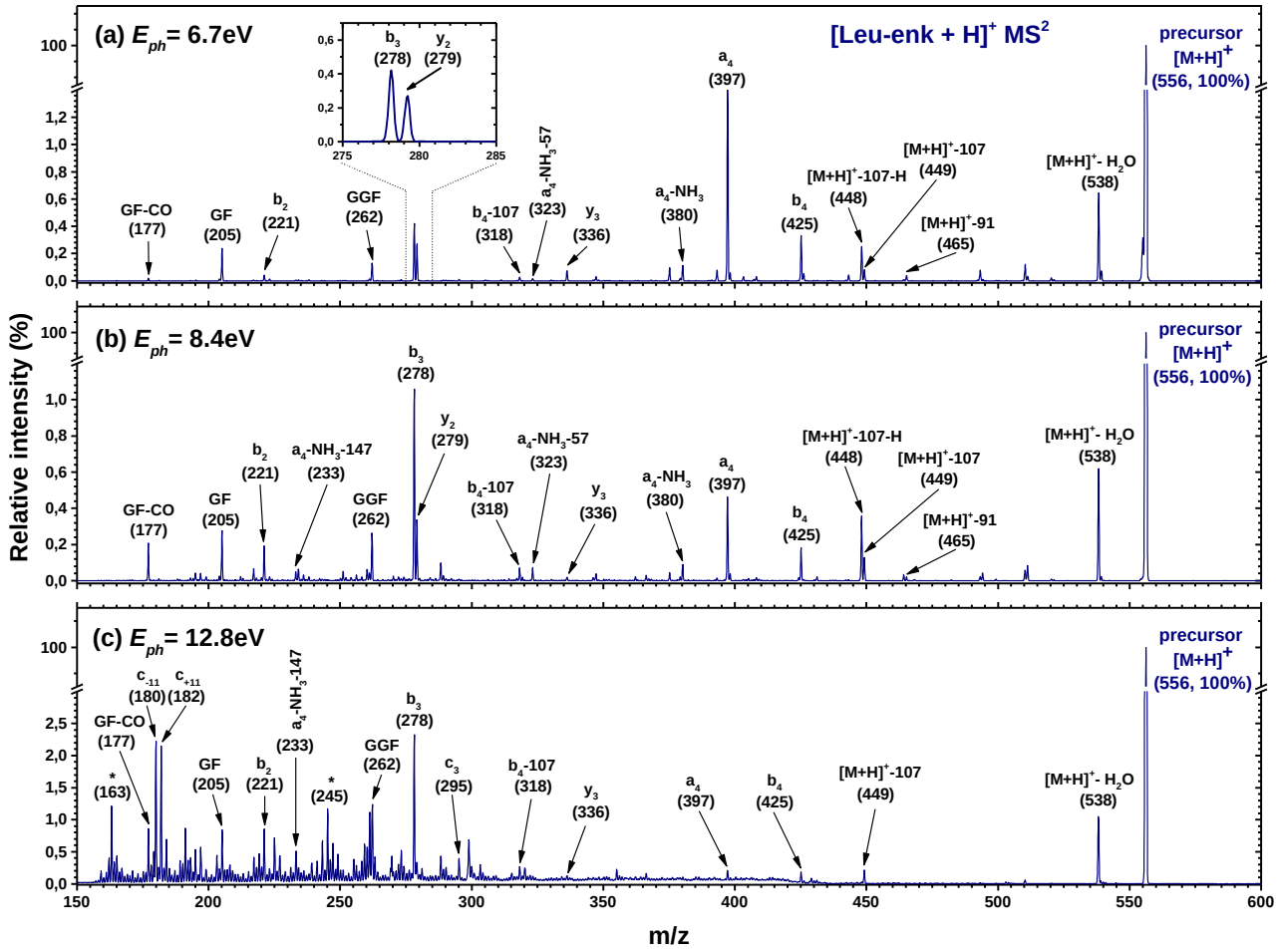

FIG. 2. Photo-activation tandem mass spectra of Leucine-enkephalin, after 500 ms irradiation of [Leu-Enk + H]$^+$ precursor at: (a) 6.7 eV, (b) 8.4 eV and (c) 12.8 eV photon energy. The proposed assignments of the most important fragments are given in the figure while "M" denotes the pseudomolecular ion.

Very similar MS^2 fragmentation patterns of present sub-IE VUV-induced dissociation (Fig. 2a,b) and CID [15] of protonated Leu-enk suggest that absorption of photons by Leu-enk molecular ions leads to electronic excitations after which intramolecular vibrational redistribution and/or internal conversion leading to a hot ground state dominantly take place. Still, it should be noted that at the energy of 8.4 eV (Fig. 2b), which is near IE, we observe a substantial change of the intensities of main peaks in the MS^2. The intensity of fragment b_3 (m/z 278) markedly increases, while quite opposite stands for the

fragments a_4 (m/z 397) and b_4 (m/z 425). The intensity of fragment GF (205) slightly increased, whereas its loss of carbon monoxide CO, namely fragment GF-CO (m/z 177), becomes stronger. Other fragments b_2 (m/z 221), GGF (m/z 262), $[M+H]^+$-107 (m/z 449) and b_4-107 (m/z 318) exhibit moderate intensity increase.

At the energy of 12.8 eV, which is well above the IE, the MS^2 spectrum significantly changes. As a result of the formation of the doubly charged radical precursor at the first instance, more fragmentation channels become open, resulting in a rich mass spectrum in the low m/z range of 150-350. Sequence fragment c_3 (m/z 295) appears. There are also unassigned fragments, which can be due to the photoionization of neutral contaminants present in the ion trap in traces. Fragments that dominated the sub-ionization mass spectrum: a_4 (m/z 397), b_4 (m/z 425) and $[M+H]^+$-107 (m/z 449) are barely visible at 12.8 eV. On the other hand, the production of the fragment corresponding to the water loss $[M+H]^+$-H_2O (m/z 538) is two-fold enhanced as compared to lower energies. After internal fragmentation of a_4-NH_3 (m/z 380), due to loss of phenylalanine residue (-147), a remaining fragment a_4-NH_3-147 (m/z 233) is also visible above IE. Doubly ionized precursor ion $[M+H]^{2+}$ (m/z 278), shows up at the same position in the mass spectrum as the fragment b_3 (278), therefore it is difficult to claim if the doubly ionized precursor can be seen in the spectrum. Even if this ion is formed, it may quickly dissociate before detection, due to a high Coulomb potential energy. In our previous work, the doubly ionized Leu-enk dimer could not be seen in the MS^2, but the nanosolvation-induced stabilization effect allowed for tracing down the doubly ionized hydrated precursor with three water molecules. In the present measurements the relative intensity of the b_3 (m/z 278) fragment increases more rapidly above the IE in comparison with other backbone fragments, as can be seen in the mass spectra presented in Fig. 2 (see also below). However, we cannot provide a definite conclusion if this is due to the contribution of $[M+H]^{2+}$ dication, formed above IE.

Present fragmentation patterns are in a very good agreement with the recent work of Bari et al. [11] in the overlapping m/z and photon energy domains. All fragments assigned in the later article [11] at the photon energy of 8 eV are also found in the present mass spectrum at the photon energy of 8.4 eV. Additionally, owing to improvement in signal to noise ratio and mass resolution, we could resolve additional important backbone fragments such as b_2, y_2, y_3, and b_4 (see Fig. 2b). Similarly, we could assign all fragments reported in ref [11] at 15 eV and resolve additional species originated from Leu-enk.

B. Photodissociation ion yields

In this section, we study the spectroscopic structures for several selected abundant fragments. This is made possible because of high signal to noise ratio and improved mass resolution for accurate and detailed measurements of desired

photofragmentation yields, in small energy steps and with a high photon energy resolution. The aim is to investigate the electronic structure of Leu-enk and specific fragmentation processes resulting from the electronic excitation. Particularly, we compare the backbone sequence specific photofragmentation yields of: a) the same type of *b* fragments (C-N bond cleavage) along the peptide backbone; b) fragments resulting from the same bond cleavage (C-N), but formed with charge left on N- or C-terminus (b_2/y_3 and b_3/y_2) and c) the fragments formed with charge rest at N-terminus, but resulting from neighboring bond cleavages (C-C_α a_4 and C-N b_4). We also compare the spectroscopic signatures of fragments resulting from detachment of different neutral groups.

Fig. 3 and Fig. 4 present selected photodissociation ion yields of singly protonated Leu-enk ion in the 5.7 to 14 eV energy range. The shown absolute uncertainties (Δ) were obtained as the biggest mismatch between overlapping points of different energy ranges, according to the normalization procedure described in the experimental section. Note however that low statistics and possible higher influence of a background in the case of very low-abundant fragments could increase the overall uncertainty of the curve shape (e.g. Fig. 3d, 8-10 eV region). The extracted ion yields show rich spectroscopic features, which will be discussed in more details below.

Fig. 3 compares relative photodissociation ion yields of the most abundant sequence specific fragments resulting from the peptide backbone dissociation. According to previous studies [18,24–27], the electronic structure of a dipeptide backbone can be described as a four-level system. Hence, the lowest energy excited states responsible for VUV photon absorption by the backbone involve: $n_0\pi_3^*$ (*W*), $\pi_2\pi_3^*$ (*NV*$_1$), $\pi_1\pi_3^*$ (*NV*$_2$) [18,24–27]. Except for the a_4 fragment (Fig. 3f), all sequence fragments presented in Fig. 3 result from cleavage of the C-N bond (*b*/*y* fragmentation). The most prominent structure in Fig. 3 is a band centered at the photon energy of about 6.9 eV. The latter band can be ascribed to the peptide $\pi_2\pi_3^*$ (*NV*$_1$) transition, most probably followed by a non-radiative decay to vibrationally excited ground state resulting in C-N bond cleavages [18]. The second band centered at about 9.6 eV clearly appears for b_3 and y_2 sequence fragments (Figs. 3b and 3e, respectively). It should correspond to the peptide $\pi_1\pi_3^*$ (*NV*$_2$) transition, followed by either direct C-N type fragmentation from the electronically excited state or upon non-radiative decay to the hot ground state [18]. The increased yield above 9 eV of all other sequence fragments shown in Fig. 3 is also notable, although it should be noted that this effect is very weak for b_4 and a_4 fragments (Figs. 3c and 3f, respectively) relative to the low-energy part. However, the second band is clearly distinguished only in the case of b_3 and y_2 fragments.

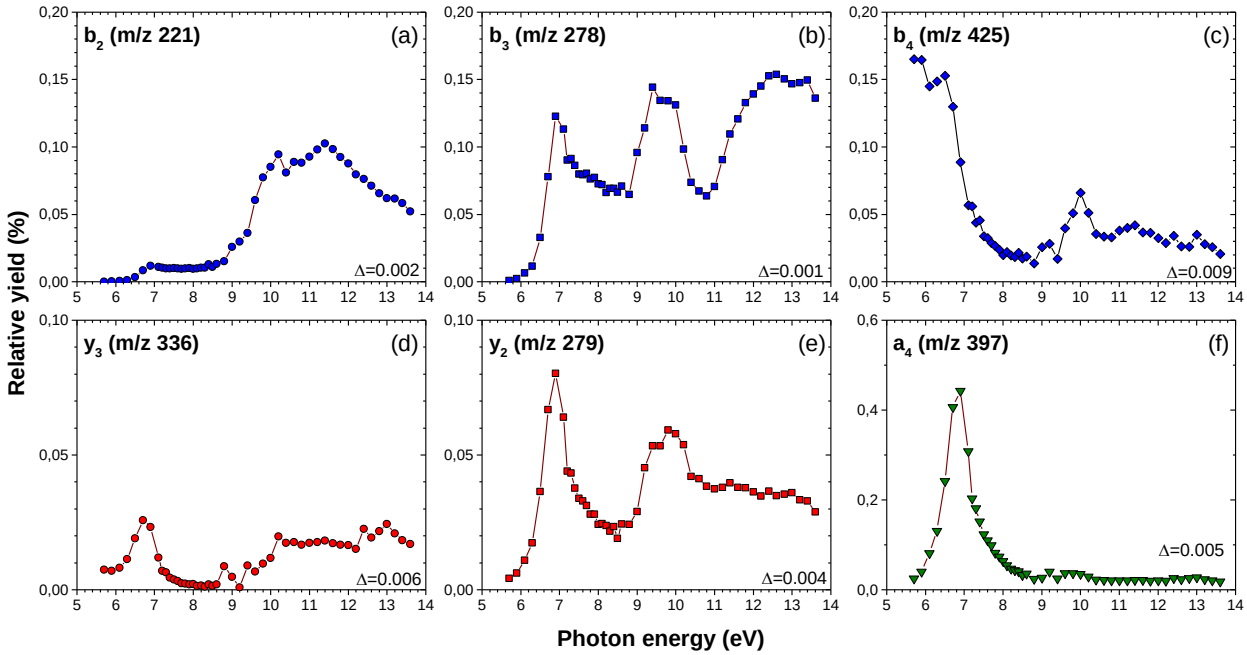

FIG. 3. Normalized relative ion yields from the photodissociation of precursor $[Leu\text{-}Enk+H]^+$ in the range of 5.7 to 14 eV. Integrated mass ranges are: (a) b_2 (m/z=220.5-221.5), (b) b_3 (m/z=277.5-278.5), (c) b_4 (m/z=424.5-425.5), (d) y_3 (m/z=335.5-336.5), (e) y_2 (m/z=278.5-279.5) and (f) a_4 (m/z=396.5-397.5). The absolute uncertainties of the experimental points obtained as the biggest mismatch between overlapping values of different energy ranges upon normalization are shown on the right bottom corner of each panel as Δ values.

According to our knowledge, there is only one existing study on VUV action spectroscopy of gas-phase Leu-enk published by Bari et al. [6] to compare with. However, Bari et al. performed measurements at only few points in the energy region overlapping with the present measurements, which cannot provide insight into the excitation bands. Still, the trends of their reported Leu-enk sequence specific fragments photodissociation yields, in the energy region 8-14 eV, are in good agreement with the present results. On the other hand, it is also interesting to compare the energy dependences of backbone dissociation for different peptides: Leu-enk (the present case) and Substance P [18]. Assuming that a peptide backbone can be generally described by a four-level electronic system, as discussed above, one would expect at least some corresponding spectroscopic features (related to photon absorption by the backbone). Indeed, the *a*-ions yield in the previous study for Substance P [18], clearly showed a band centered at about 6.8 eV that compares very well with the present a_4-ion yield (Fig. 3f). The additional higher-energy structures are also visible for *a*-ions, as well as *x*, *b* and *y* ions in the previous study [18] above 8 eV and peaking somewhere between 10 and 12 eV. The later features may correspond to the present band at about 9.6 eV, as well as broad features found for *b* and *y* fragments above 10 eV. However, it is interesting that in the previous study of Substance P, *b* fragments appear only above about 8 eV, while in the present case of protonated Leu-enk, there is a very strong band for *b* fragments at the energy of 6.9 eV, as found for the *a* fragment. Moreover, even in the case of *a* and *y* fragments of Substance P, where the first 6.9 eV band can be clearly resolved, its intensity is still considerably inferior to the

signal above 8 eV. In contrast, for Leu-enk, the band at 6.9 eV represents a dominant feature for most of the *b* and *y* fragments spectra and particularly for the a_4 fragment. In a previous study, González-Magaña *et al.* [28] have reported an effect of the peptide chain length on the fragmentation patterns. Short peptides bearing up to 7 residues appeared to have a different behavior than longer one (with 12 residues), which was assigned to charge migration following photoionization. In the present case, we also observe a very different photochemistry below the ionization threshold for Leu-Enk (5 residues) with respect to Substance P (11 residues).

Figs. 3a, b and c (blue curves – in the first raw) present VUV photodissociation yields of *b* fragments (cleavage of C-N bond with charge left on N-terminus). The later offer an exciting insight into the energy dependence of the cleavage of the peptide linkage as a function of its site along the Leu-enk peptide backbone. Since all *b* yields correspond to the same C-N bond cleavage, their different energy dependences steam from different VUV absorption efficiency, which correspond to the change of the electronic density of the biopolymer along its backbone. Indeed, Figs. a-c show that the relative ion yields strongly depend on the position of the C-N bond cleavage on the peptide. Clearly, with approaching C-terminus (and increasing the fragment size) the low-energy part of the action spectra becomes more important. Particularly, the low-energy absorption at about 6.9 eV, assigned to NV_1 electronic transition, appears to be weak for b_2 fragment (Fig. 3a) relative to the fragmentation intensity at photon energies above 8 eV, which is very similar to the previous case found for Substance P. However, already for b_3 fragment (Fig. 3b) the 6.9 eV band is very strong. Moreover, for b_4 fragment (Fig. 3c) the photodissociation yield still increases with decreasing the photon energy below 6 eV suggesting that peptide dissociation to b_4 may be triggered even by the lowest energy $n_0\pi_3^*$ (*W*) transition previously suggested to be at about 5.5 eV [18]. VUV photodissociation to *b* and *y*-type fragments of protonated Substance P has not been observed below 6 eV, although it was reported for *a*-type fragments. Still, it is interesting to note that the present b_2 relative photodissociation yield corresponds very well to the measured energy dependences for small neutral losses; for example $-H_2O$ in the present case of protonated Leu-enk (Fig. 4b), or $-NH_3$ in the previously investigated Substance P [18]. Significant differences in relative photodissociation yields corresponding to a same bond cleavage along the peptide backbone, suggest a strong influence of the protonation site to the frontier peptide orbitals and a redistribution of the electronic density along the peptide backbone upon protonation.

The present results also offer a possibility to compare the photodissociation yields of different fragments that are directly produced by the cleavage of the same bond (see Fig. 1). In Fig. 3, we compare the yields of b_2 (a) and y_3 (d), as well as of b_3 (b) and y_2 (e). A pair of fragments produced by the same bond scission is expected to have similar photodissociation yields, which is indeed shown in Fig. 3 for b_2/y_3 and b_3/y_2. Still, it is interesting that in both cases *y* fragments appear to have

somewhat higher relative intensity at lower photon energies. The other notable difference is a strong increase of b_3 fragment yield above 11 eV (Fig. 3b), which is not seen for the corresponding y_2 fragment (Fig. 3e). It has been already noted above that b_3 (m/z 278) cannot be resolved from the doubly charged precursor $[M+H]^{2+}$, which should strongly increase above the IE. However, the doubly charged precursor may not survive until detection. Finally, for both pairs of *b*/*y* fragments, the abundance of *b* fragments is much higher over the whole photon energy range, which is expected since N-terminus should represent the preferential protonation site of the gas-phase protonated Leu-enk [29].

In the last column of Fig. 3, we compare the photodissociation yields of fragments produced by cleavage of neighboring bonds from the same carboxyl C atom (see Fig. 1), and with the charge left on N-terminus; namely, b_4 (Fig. 3c) is produced by a C-N cleavage and a_4 (Fig. 3f) is produced by a C_α-C cleavage. Clearly, in both cases, fragmentation into these ionic species dominantly occurs at low photon energies. The formation of the later fragments is preferentially triggered by $\pi\pi^*$ electronic transitions. Both dissociation yields show a strong band at about 6.9 eV, as well as an increased yield at photon energies between 9 and 10.5 eV. The a_4 fragment is significantly more abundant at low energies and its action spectrum shows a strong absorption band centered at about 6.9 eV, which is typically seen for most of the other fragments. However, interestingly, the C_α-C bond cleavage producing a_4 does not seem to be important below 6 eV, in contrast to the cleavage of closely situated C-N bond producing b_4.

Besides sequence specific fragments, we also study the energy dependence of the formation of fragments involving multiple bonds breaking and neutral losses. In Fig. 4, we compare photodissociation yields of the fragment GF (m/z 205) with the fragments produced by loss of the water molecule (m/z 538) and the tyrosine side chain (m/z 449). According to the previous study, the formation of GF fragment is not associated with substantial rearrangements of the system and proceeds along entropically favored pathway [30]. Furthermore, it has been suggested according to the same surface-induced dissociation study [30] that GF fragment was formed from y_3 (mainly) and a_4 fragments. Therefore, one would expect that significant formation of GF can occur already at lower VUV photon energies below the IE and that the relative photodissociation yield of GF (Fig. 4a) is similar to the yields of y_3 (Fig. 3d) and a_4 (Fig. 3f). Indeed, the dominant feature for GF yield appears at about 6.9 eV (assigned above to NV_1), as found for y_3 and particularly for a_4. Also, as for y_3 and a_4, additional features can be seen between 9 and 10.5 eV (assigned to NV_2). However, it is interesting to note that, in contrast to y_3 and a_4, the yield of GF strongly increases above the IE. We can therefore, tentatively explain the depletion of *b*, *y* and *a* fragments at higher photon energies as being due to increased formation of other, internal fragments. In this particular case for example, GF represents a

favored channel at higher photon energies. Note that this domination is even more pronounced with the further increase of the photon energy above 14 eV [31].

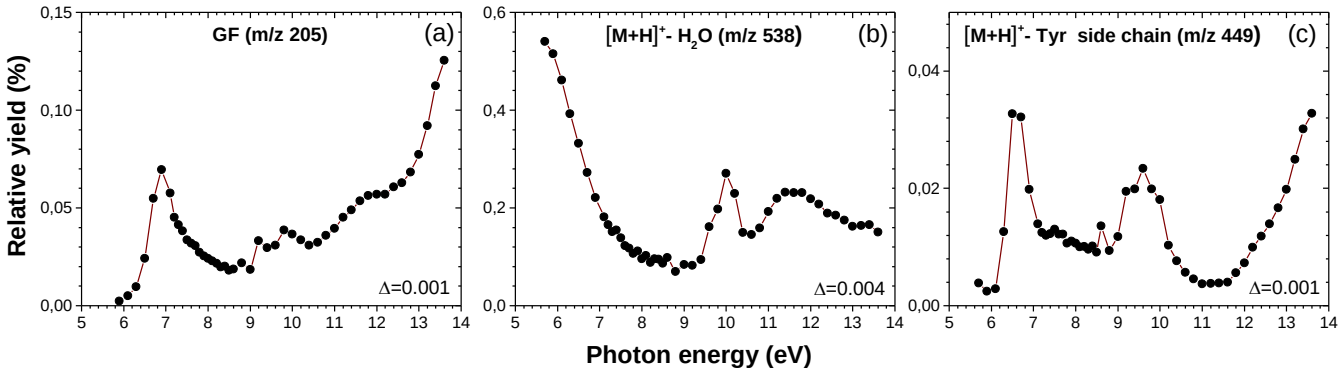

FIG. 4. Normalized relative ion yields from the photodissociation of precursor $[Leu\text{-}Enk+H]^+$ in the range of 5.9 to 14 eV. Integrated mass ranges are: (a) GF (m/z=203.5-204.5), (b) $[M+H]^+$-H_2O (m/z=537.5-538.5) and (c) $[M+H]^+$-tyrosine side chain (m/z=448.5-449.5).

The loss of the water molecule from protonated Leu-enk has been detected as a relatively strong fragmentation channel upon both CID [15] and surface-induced dissociation [30], but this process was not discussed in details. Moreover, in the previous study of VUV photodissociation of protonated Leu-enk by Bari et al. [11], the fragment formed upon loss of water was above the m/z cutoff presented by the authors. Therefore, according to our knowledge, we report for the first time the energy dependence of VUV-induced loss of water from protonated Leu-enk peptide. Interestingly, the present study shows (Fig. 4b) that $-H_2O$ photodissociation yield appears to be markedly different at low photon energies from the yields of other neutral losses (Fig. 4c), internal fragment GF (Fig. 4a) and sequence fragments (Fig. 3), except for the b_4 fragment yield which curve also show an intense abundance at low photon energy, well below the 6.9 eV band. Therefore, we can tentatively assume that loss of water can proceed from the lowest $n_0\pi_3^*$ (*W*) peptide excitation, similarly as for b_4 fragment. Note that b_4 fragment is formed by the cleavage of the C-N bond close to the C-terminal of Leu-enk, so in close vicinity to a carboxyl group, which could be the site from where the water molecule is extracted. It should be noted that a similar strong increase of the yield towards low photon energies, has been seen for a small methionine residue loss (-15) in the previous study with Substance P [18], however methionine absorbs at rather low energies in contrast to carbonyl chromophores.

The loss of tyrosine side chain has been already studied before[11] but with large energy steps. The present results discover a rich spectroscopic structure corresponding to protonated Leu-enk dissociation to this fragment. Two bands are clearly resolved at about 6.9 eV and 9.8 eV. With this respect, the spectrum is comparable with *b* and *y* sequence fragments (Fig. 3),

suggesting that loss of Tyr side chain can be triggered by backbone photon absorption. The spectrum is similar to most of the neutral losses from Sub P.

IV. CONCLUSION

We presented a detailed study on energy dependent fragmentation of protonated Leu-enk peptide in the VUV photon domain from 5.7 eV (217.5 nm) to 14 eV (88.56 nm) with unprecedented spectral details, owing to the very small steps between the photon energies. The fragment ion yields exhibit rich features, which have been assigned to excitation of the lowest energy excited states. The most prominent structure appeared at the photon energy of about 6.9 eV. The latter band is ascribed to the peptide $\pi_2\pi_3^*$ (*NV1*) transition. The fragmentation pattern at low photon energy is similar to that produced under CID excitation conditions. Thus, based on this argument, we propose that the photofragmentation below the threshold proceed on the hot ground electronic state after internal conversion. However, we have also found significant differences between relative photodissociation yields that correspond to the cleavage of the C-N bond along the peptide backbone. Moreover, interestingly, the photochemical behavior of protonated Leu-enk is very different from the one reported recently for substance P. This observation is in line with previous investigations on the length effects on VUV fragmentation of peptides [28]. Although the origin of such differences is not yet explained and requires further work, it clearly appears that the photochemical and photophysical properties of small peptides cannot be simply extended and serve as model to longer systems such as bigger peptides and proteins. Indeed, there is a strong interplay between the length of a biopolymer and its electronic structure.

---

[a] Author to whom correspondence should be addressed. Electronic mail: vraz@ipb.ac.rs.

ACKNOWLEDGMENTS

This work was supported by the Agence Nationale de la Recherche, France, under project ANR-08-BLAN-0065. M.LJ.R. and A.R.M. acknowledge support by the Ministry of Education, Science and Technological Development of Republic of Serbia under project #171020. The Notre Dame Radiation Laboratory is supported by the U.S. Department of Energy Office of Science, Office of Basic Energy Sciences under Award Number DE-FC02-04ER15533 (this is document number NDRL 5093). We thank the general staff of the SOLEIL synchrotron radiation facility, for running the beam smoothly and for providing beamtime under project 20131031.

REFERENCES

[1] Christian B. Anfinsen, Science (80-.). **181**, 223 (1973).

[2] O. Plekan, V. Feyer, R. Richter, M. Coreno, M. De Simone, K.C. Prince, and V. Carravetta, J. Phys. Chem. A **111**, 10998 (2007).

[3] F. Gaie-Levrel, G. a Garcia, M. Schwell, and L. Nahon, Phys. Chem. Chem. Phys. **13**, 7024 (2011).

[4] M. Tia, B. Cunha de Miranda, S. Daly, F. Gaie-Levrel, G.A. Garcia, L. Nahon, and I. Powis, J. Phys. Chem. A **118**, 2765 (2014).

[5] K.R. Wilson, M. Jimenez-Cruz, C. Nicolas, L. Belau, S.R. Leone, and M. Ahmed, J. Phys. Chem. A **110**, 2106 (2006).

[6] M. Schwell and M. Hochlaf, Top. Curr. Chem. **355**, 155 (2015).

[7] L. Belau, K.R. Wilson, S.R. Leone, and M. Ahmed, J. Phys. Chem. A **111**, 7562 (2007).

[8] E. Pluhařová, P. Slavíček, and P. Jungwirth, Acc. Chem. Res. **48**, 1209 (2015).

[9] J.-W. Ho, H.-C. Yen, H.-Q. Shi, L.-H. Cheng, C.-N. Weng, W.-K. Chou, C.-C. Chiu, and P.-Y. Cheng, Angew. Chemie Int. Ed. **54**, 14772 (2015).

[10] A.R. Milosavljević, C. Nicolas, J. Lemaire, C. Dehon, R. Thissen, J.-M. Bizau, M. Réfrégiers, L. Nahon, and A. Giuliani, Phys. Chem. Chem. Phys. **13**, 15432 (2011).

[11] S. Bari, O. Gonzalez-Magaña, G. Reitsma, J. Werner, S. Schippers, R. Hoekstra, and T. Schlathölter, J. Chem. Phys. **134**, 024314 (2011).

[12] A. Giuliani, A.R. Milosavljević, F. Canon, and L. Nahon, Mass Spectrom. Rev. **33**, 424 (2014).

[13] C. Brunet, R. Antoine, A.-R. Allouche, P. Dugourd, F. Canon, A. Giuliani, and L. Nahon, J. Phys. Chem. A **115**, 8933 (2011).

[14] P. Kebarle and U.H. Verkerk, Mass Spectrom. Rev. **28**, 898 (2009).

[15] K.V. Judit Sztáray, Antony Memboeuf, László Drahos, Mass Spectrom. Rev. **30**, 298 (2011).

[16] A.R. Milosavljević, V.Z. Cerovski, F. Canon, L. Nahon, and A. Giuliani, Angew. Chem. Int. Ed. Engl. **52**, 7286 (2013).

[17] A.R. Milosavljević, V.Z. Cerovski, M.L. Ranković, F. Canon, L. Nahon, and A. Giuliani, Eur. Phys. J. D **68**, 68 (2014).

[18] F. Canon, A.R. Milosavljevic, L. Nahon, and A. Giuliani, Phys. Chem. Chem. Phys. **17**, 25725 (2015).

[19] A.R. Milosavljević, C. Nicolas, J.-F. Gil, F. Canon, M. Réfrégiers, L. Nahon, and A. Giuliani, J. Synchrotron Radiat. **19**, 174 (2012).

[20] L. Nahon, N. de Oliveira, G. a Garcia, J.-F. Gil, B. Pilette, O. Marcouillé, B. Lagarde, and F. Polack, J. Synchrotron Radiat. **19**, 508 (2012).

[21] A.R. Milosavljević, C. Nicolas, J.-F. Gil, F. Canon, M. Réfrégiers, L. Nahon, and A. Giuliani, Nucl. Instruments Methods Phys. Res. Sect. B Beam Interact. with Mater. Atoms **279**, 34 (2012).

[22] K. Biemann, Methods Enzymol. **193**, 455 (1990).

[23] P. Roepstorff and J. Fohlman, Biomed. Mass Spectrom. **11**, 601 (1984).

[24] L. Serrano-Andrés and M.P. Fülscher, J. Am. Chem. Soc. **118**, 12190 (1996).

[25] L. Serrano-Andrés and M.P. Fülscher, J. Am. Chem. Soc. **118**, 12200 (1996).

[26] L. Serrano-Andrés and M.P. Fülscher, J. Am. Chem. Soc. **120**, 10912 (1998).

[27] L. Serrano-Andrés and M.P. Fülscher, J. Phys. Chem. B **105**, 9323 (2001).

[28] O. González-Magaña, G. Reitsma, S. Bari, R. Hoekstra, and T. Schlathölter, Phys. Chem. Chem. Phys. **14**, 4351 (2012).

[29] N.C. Polfer, J. Oomens, S. Suhai, and B. Paizs, J. Am. Chem. Soc. **129**, 5887 (2007).

[30] J. Laskin, J. Phys. Chem. A **110**, 8554 (2006).

[31] M.Lj. Ranković, F. Canon, L. Nahon, A. Giuliani, and A.R. Milosavljević, J. Phys. Conf. Ser. **012034**, 4 (2015).